3-1-2018

An Efficient Coal Pyrolysis Model for Detailed Tar Species Vaporization

Jianqing Li
Marquette University

Simcha L. Singer
Marquette University, simcha.singer@marquette.edu

Accepted version. *Fuel Processing Technology*, Vol. 171 (March 2018): 248-257. DOI.

Fuel Processing Technology, Vol. 171 (March 2018): 248-257. DOI.

Contents

Abstract 2

Keywords 2

1. Introduction 2

2. Tar vaporization model 4

2.1. Discrete component model 4

2.1.1. Vapor-liquid equilibrium in CPD 4

2.1.2. Rate-based VLE model 5

2.1.3. Vapor-liquid equilibrium in FLASHCHAIN 6

2.2. Direct quadrature method of moments 6

2.3. Delumping model 10

3. Test case 12

3.1. Modified CPD model 12

3.2. Numerical approach 13

4. Results and discussion 13

5. Conclusions 18

Nomenclature 18

Subscripts 19

Acknowledgments 19

References 19

An Efficient Coal Pyrolysis Model for Detailed Tar Species Vaporization

Jianqing Li
Department of Mechanical Engineering, Marquette University, Milwaukee, WI
Simcha L. Singer
Department of Mechanical Engineering, Marquette University, Milwaukee, WI

Abstract

An accurate and computationally efficient model for the vaporization of many tar species during coal particle pyrolysis has been developed. Like previous models, the molecular fragments generated by thermal decomposition are partitioned into liquid metaplast, which remains in the particle, and vapor, which escapes as tar, using a vapor-liquid equilibrium (VLE) sub-model. Multicomponent VLE is formulated as a rate-based process, which results in an ordinary differential equation (ODE) for every species. To reduce the computational expense of solving many ODEs, the model treats tar and metaplast species as a continuous distribution of molecular weight. To improve upon the accuracy of previous continuous thermodynamic approaches for pyrolysis, the direct quadrature method of moments (DQMoM) is proposed to solve for the evolving distributions without assuming any functional form. An inexpensive delumping procedure is also utilized to recover the time-dependent mole fractions and fluxes for every discrete species. The model is well-suited for coal-to-chemicals processes, and any application which requires information on a range of tar species. Using a modified CPD model as the basis for implementation of the VLE submodel, agreement between the full discrete model and DQMoM with delumping is excellent, with substantial computational savings.

Keywords

Coal, Pyrolysism Vaporization, Continuous thermodynamics, Direct quadrature method of moments (DQMoM), Delumping

1. Introduction

Pyrolysis is the thermal decomposition of a solid fuel, such as coal or biomass, which produces gaseous, liquid and solid products. As a coal particle is heated, its macromolecular structure begins to decompose, creating a wide range of molecular fragments and light gases. A portion of the molecular fragments are released from the particle as tar, and together with the light gases, comprise the volatiles. Hundreds of light gas and tar species are produced during coal pyrolysis.[1,2] While pyrolysis (or devolatilization, in the presence of oxygen) occurs as the initial step during coal combustion and gasification, pyrolysis as a stand-alone process can be used for the production of chemicals and fuels from coal.[1] Knowledge of the tar compounds formed during pyrolysis is important for such coal-to-chemicals processes, as well as for predicting soot formation during coal gasification and combustion by pairing with an elementary reaction mechanism.[3]

A range of pyrolysis models have been developed. Single-step models are typically valid only under the conditions for which their kinetic constants have been determined. Distributed activation energy models use Arrhenius rates with a distribution of activation energies to represent the numerous chemical pathways for production of volatiles from coal's complex macromolecular network.[4] The most accurate models are the comprehensive models that account for the coal's molecular structure:[5] Chemical Percolation Devolatilization (CPD),[6] FLASHCHAIN[7] and FG-DVC.[8] These models are based on a realistic description of a coal's structure, a mechanistic description of its disintegration upon heating, the release of light gases, cross-linking of metaplast and the vaporization of molecular fragments as tar. The tar vaporization model in CPD is based on the flash equilibrium analogy originally developed in a precursor to FLASHCHAIN,[9] which is more accurate than the vaporization submodel in FG-DVC.

Rather than predicting the production of individual tar species, CPD and FLASHCHAIN predict the production of lumped tar species as a function of molecular weight. In the CPD model, fragment species are lumped into discrete groups, with each lump typically comprising species with a range of roughly 300 kg/kmol.[10,11] This approach is an example of a discrete component model (DCM), employing quasi-components rather than discrete species. FLASHTWO, a precursor to FLASHCHAIN, assumed that the fragment molecular weights followed a continuous gamma distribution and calculated the evolution of the distribution's parameters with time,[9] or specified the distribution to fit experimental data.[12] Treating the species as a continuous distribution constitutes a continuous thermodynamic model (CTM).[13] However, due to the inaccuracy associated with specifying the distribution function a priori throughout pyrolysis, FLASHCHAIN calculates the fragment distribution from population balance equations for each fragment size,[7] which can again be considered a quasi-DCM, as in CPD.

In general, for problems governed by differential equations, DCM approaches yield information on every discrete (or quasi-discrete) species but can become computationally intensive when the number of species becomes large. CTM approaches are computationally efficient, but can be less accurate due to the assumption of the form of the distribution function, and only provide information on the distribution, rather than on individual species.

This paper presents an accurate and efficient CTM for tar vaporization during coal pyrolysis, as well as a delumping step which combines the advantages of DCMs and CTMs. To remove the computational time-step dependence[11] in the CPD VLE model, the vaporization process is treated as a rate-based process,[14] as in FLASHCHAIN.[7] However, rather than solving an ordinary differential equation for every discrete or quasi-discrete species, a CTM is employed, as in FLASHTWO.[9] The first novelty of the model presented is that rather than using a continuous distribution function that is specified a priori,[9] the Direct Quadrature Method of Moments (DQMoM) is used to efficiently and accurately solve for the evolution of the distribution of tar and metaplast species without assuming any functional form. The second novelty is an accurate and inexpensive delumping procedure that is used to recover the time-dependent mole fractions and fluxes for every discrete tar and metaplast species, providing the same information as a DCM at a significantly reduced computational cost.

The tar vaporization model described in this paper is well-suited to kinetic models which produce many tar species. Molecular dynamics simulations have recently been applied to coal pyrolysis to predict individual reaction products for a variety of coals,[15,16,17] represented by large-scale coal models.[18,19] However, these simulations have not yet included models to partition the molecular fragments generated into tar (vapor) and metaplast (liquid) and simulate very short periods of time. Recently, an extension of the CPD model has been developed that can predict the formation of specific tar compounds.[3] Future models might combine the advantages of these two simulation approaches, parametrizing kinetic schemes based on functional groups[8,20] with detailed species information obtained from molecular dynamics simulations. DQMoM for tar vaporization is applicable to any kinetic scheme for macromolecular decomposition, while application of the delumping procedure is restricted to models without reactions between individual metaplast species, such as the biomolecular recombination reactions in FLASHCHAIN.[7]

The rate-based tar vaporization model is presented in discrete form in Section 2.1. The discrete version of the model is computationally expensive if applied to many species. Section 2.2 describes the DQMoM approach for coal tar vaporization and the delumping procedure is outlined in Section 2.3. The test case for the model is based on a modified version of the CPD model and is described in Section 3. Results and discussion comparing the DQMoM and delumping models to the DCM are presented in Section 4, with conclusions in Section 5.

2. Tar vaporization model

2.1. Discrete component model

2.1.1. Vapor-liquid equilibrium in CPD

The vapor-liquid equilibrium (VLE) submodel in the CPD model applies Raoult's Law to relate the liquid (x_i) and vapor (y_i) mole fractions of a quasi-discrete fragment species, *i*,

$$(1)\ y_i = K_i x_i$$

and the nonlinear Rachford-Rice equation to calculate the phase of molecular fragments generated from decomposition of the macromolecular structure.[11] The VLE equilibrium constant, K_i, in Raoult's Law is a function of molecular weight and temperature, and a correlation with parameters α, β and γ is based on a wide range of vapor pressures:[21]

$$(2)\ K_i \equiv \frac{P_i^v}{P} = \frac{\alpha exp\left(-\beta MW_i^\gamma / T\right)}{P}$$

The Rachford-Rice approach used in the CPD model assumes that VLE occurs as a batch process (Fig. 1a): the fragments and light gas generated via decomposition during the last time step are combined with the fragments that have accumulated in the metaplast over all previous time steps to calculate, f_i, the "feed" of lumped fragments, *i*, which enters the flash vessel. This approach has the disadvantage that the equations depend on the numerical time step, a fact recognized by the developers of the CPD model:[11] longer time steps result in more light fragments and gas in the feed, while shorter time steps result in a feed consisting mostly of heavy species that have accumulated in the metaplast. The instantaneous vapor-to-feed ratio, *V*/*F*, computed from the Rachford-Rice equation, is heavily dependent on the time-step.[14] Nonetheless, in the CPD model, the computational time step does not have a significant impact on the calculation of mass fractions of tar and gas. This is because the average molecular weight of each lumped fragment differs from the next biggest/smallest lump by ~ 300 amu, so whether *V*/*F* is small or large during a particular time step doesn't change the results appreciably; heavy species with $K_i \ll 1$ will remain in the particle, while light species with $K_i \gg 1$ will vaporize.[14] However, it cannot be assumed that the time step dependence will not impact the solution when many species with similar molecular weights are present. For this reason, the current VLE model employs a rate-based process (Fig. 1b), similar to the VLE in FLASHCHAIN[7] (see Section 2.1.3).

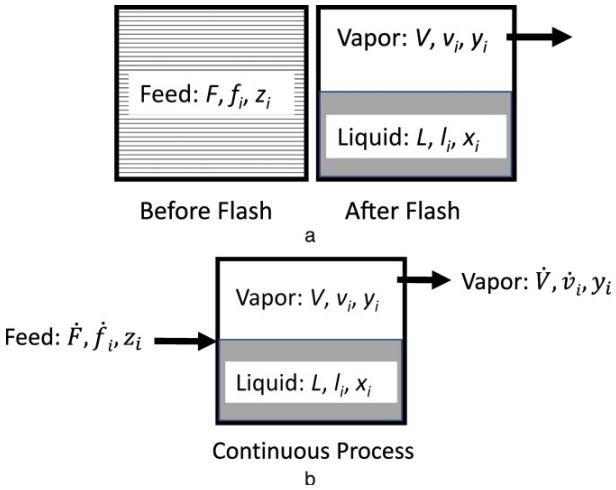

Fig. 1. (a) Vapor-liquid equilibrium as a batch process, and (b) as a continuous process.

2.1.2. Rate-based VLE model

Applying a total mole balance to the flash vessel (coal particle) shown in Fig. 1(b) for a continuous process, and accounting for the depletion of liquid species via crosslinking as in the CPD model, yields

$$(3)\ \frac{dL}{dt} = \dot{F} - \dot{V} - k_{cross}L - \frac{dV}{dt}$$

where L is the total moles of liquid in the particle, V is the total moles of vapor in the particle, $\dot{F}$ is the total molar flow rate at which the fragments are generated from decomposition reactions, $\dot{V}$ is the total vapor flow rate leaving the particle and k_{cross} represents the rate constant for crosslinking of liquid to solid char, and is the same for all tar species. Although the dV/dt term is often negligible, it is retained in the equation for generality as discussed below. Assuming minimal pressure rise in the particle,[9] and using the ideal gas law, dV/dt depends on the rate of change of the particle's temperature.

Applying a molar balance to each discrete or quasi-discrete species results in:

$$(4)\ \frac{dl_i}{dt} + \frac{dv_i}{dt} = z_i\dot{F} - y_i\dot{V} - x_i k_{cross}L$$

where l_i is the moles of liquid i in the particle, v_i is the moles of vapor i in the particle, x_i is the mole fraction of i in the liquid phase, y_i is the mole fraction of $i$in the vapor phase calculated using Eqs. (1), (2), and z_i is the mole fraction of i in the feed (generated by decomposition reactions). Expanding terms, combining with the total mole balance and rearranging yields the governing equation for each species mole fraction, x_i, in the liquid phase:

$$(5)\ \frac{dx_i}{dt} = \left[\frac{(z_i - x_i)\dot{F}}{L + VK_i} + \frac{x_i(1-K_i)\dot{V}}{L+VK_i} - \frac{Vx_i}{L+VK_i}\frac{dK_i}{dt} + \frac{x_i(1-K_i)}{L+VK_i}\frac{dV}{dt}\right]$$

Finally, the total vapor molar flow rate, $\dot{V}$, is obtained from the algebraic constraint that the vapor mole fractions sum to unity.[22]

$$(6)\ \sum_i y_i = 1$$

Eqs. (3), (5), (6) represent a non-linear system of differential-algebraic equations (DAEs). The nonlinearity stems from the dependence of $\dot{V}$ on the x_i. This can be seen by differentiating Eq. (6) until it becomes an explicit equation for $\dot{V}$, although solving the system as one of ODEs rather than treating the system as one of DAEs leads to drift-off error.[23]

2.1.3. Vapor-liquid equilibrium in FLASHCHAIN

VLE in FLASHCHAIN is also treated as a rate-based process. In FLASHCHAIN it is assumed that there is no accumulation of any vapor species within the particle.[9] With this assumption, the governing equations in the model reduce to

$$(7)\ \frac{dL}{dt} = \dot{F} - \dot{V} - k_{cross}L$$

$$(8)\ \frac{dx_i}{dt} = \left[\frac{(z_i - x_i)\dot{F}}{L} + \frac{x_i(1-K_i)\dot{V}}{L}\right]$$

and the total vapor molar flow rate, $\dot{V}$, can be obtained explicitly from the light gas generation rate.[7]

$$(9)\ \dot{V} = \frac{\dot{v}_{gas}}{y_{gas}} = \frac{\dot{f}_{gas}}{1-\sum_{i\neq gas} K_i x_i}$$

Substituting Eqs. (9), (8) again results in a non-linear system, like Eqs. (3), (5), (6), but is one of ODEs rather than DAEs.

The computationally efficient DQMoM approach proposed in this paper is applicable to both the DAE and ODE versions of the VLE model, Eqs. (3), (5), (6), or Eqs. (7), (8), (9), respectively. Niksa performed a scaling analysis and concluded that accumulation of vapor species in coal particles is negligible.[9] The form of the distribution function therein was fixed and was excluded from the time derivative in the governing equation, which leads to omission of some terms in Eq. (5). Comparing the DAE and ODE versions of the VLE for the test case presented in Section 3 resulted in a relative root mean square difference of 3.47% in tar vaporization rates. For higher heating rates and pyrolysistemperatures than used in the test case, rapid changes in temperature (large dT/dt) could cause accumulation or depletion of vapor species, or the dK_i/dtterms, to be more significant. DQMoM and delumping will therefore be demonstrated with the more general DAE version of the model, Eqs. (3), (5), (6), although this version has a higher computation time than the ODE version for both DQMoM and the full DCM approach.

2.2. Direct quadrature method of moments

During coal pyrolysis, hundreds of molecular fragments are generated.[1,2] However, calculating the detailed species distribution that escapes the particle as tar would be extremely computationally expensive, as Eq. (5) must be solved for every species. In practice, in CPD[11] and FLASHCHAIN,[24] tar species are lumped into different fragment sizes, generally using relatively coarse bins. An alternative approach is to represent the species as a *continuous* distribution of molecular weight instead of solving ODEs for each species.[9] In this paper, DQMoM is proposed to solve for the evolution of the tar and metaplast distributions accurately and efficiently, without assuming any functional form.

Cotterman et al. developed continuous thermodynamic models (CTM) and semi-continuous thermodynamic models to treat a multicomponent mixture as a prescribed continuous function of boiling point or molecular weight.[13,25] Lage[26] applied the Quadrature Method of Moments (QMoM)[27] to allow a continuous mixture's distribution to evolve into any functional form. In the context of multicomponent droplet vaporization, Bruyat et al.[28] applied the Direct Quadrature Method of Moments (DQMoM)[29] in place of QMoM, due to its mathematical equivalence and computational stability. For certain problems, a CTM may be “delumped” to provide information on all discrete species with negligible computational expense, combining the advantages of CTMs and DCMs in a single method.[30,31]

DQMoM will be applied to tar/metaplast vapor-liquid-equilibrium during coal pyrolysis, and its accuracy and computational cost will be compared to the alternative of solving for every discrete species using a full DCM, represented by Eq. (5). A semi-continuous formulation[25] will be employed, as the light gas which dominates the vapor phase will be considered separately. The molecular weight is chosen as the distribution variable for the tar/metaplast because the correlation for vapor pressure is given in terms of molecular weight.[11] It would also be possible to use DQMoM for multiple distributions, each representing distinct chemical families within the tar, if different correlations were to be used for each chemical family. Because the method has not been previously applied to pyrolysis models, the development of (D)QMoM is outlined below.

QMoM solves for the time evolution of a distribution by tracking several of its moments[27] and has been applied to a variety of problems.[27,32,33,34] QMoM treats the governing discrete equation, in this case Eq. (5), as a continuous equation

$$\frac{dx(I,t)}{dt} = S(I,t) \tag{10}$$

where $x(I, t)$ represents the continuous distribution of liquid mole fractions as a function of the "internal variable," I, which represents the molecular weight, and time, t. The source term, $S(I, t)$, represents the continuous version of the right-hand-side of Eq. (5). QMoM multiplies both sides of Eq. (10) by I^k, for $k = 0{:}2N - 1$, and integrates from 0 to ∞, to transform the governing continuous equation into an equation for the first $2N$ moments, m_k, of the evolving distribution,[27]

$$\frac{dm_k}{dt} = \overline{S_k} \tag{11}$$

where the transformed source term is

$$\overline{S_k} = \int_0^\infty S(I,t) I^k dI \tag{12}$$

It is possible to write the integrand as,

$$\int_0^\infty S(I) I^k dI = \int_0^\infty x(I) f(I) dI \tag{13}$$

treating the distribution as a weight function and using a Gaussian quadrature to evaluate the integral without introducing any higher order moments:[35]

$$\int_0^\infty x(I) f(I) dI \approx \sum_{j=1}^{N} w_j f(I_j) \tag{14}$$

w_j and I_j are, respectively, the weights (mole fractions) and nodes (molecular weights) of the quadrature, and N is the number of nodes used in the interpolation formula.

QMoM allows for the evolution of an arbitrarily shaped distribution and the accuracy of the approximation is typically quite good with only a few nodes. However, computation of the time-dependent weights and nodes, w_j and I_j, requires application of the product-difference algorithm[36] or Wheeler's algorithm[37] at every time step, potentially leading to instability.

The Direct Quadrature Method of Moment (DQMoM) is mathematically equivalent to QMoM for univariate distributions, but solves directly for the weights and nodes in Eq. (14).[29] Numerically, DQMoM is often more stable than QMoM[28] and can be more convenient for pairing with other equations solved with a standard ODE or DAE solver.

The Gaussian quadrature of Eq. (14) is mathematically equivalent to treating the distribution as a summation of N delta functions at nodes I_j and with weights w_j:[29]

(15)

$$x(I,t) = \sum_{j=1}^{N} w_j(t)\delta\left[I - I_j(t)\right]$$

Combining Eq. (15) with the governing Eq. (10) results in:

(16)

$$\sum_{j=1}^{N} \frac{\partial}{\partial t}\left[w_j \delta\left(I - I_j\right)\right] = S(I,t)$$

The left hand side can be expanded using derivative rules to arrive at:[35]

(17)

$$\sum_{j=1}^{N} \delta\left(I - I_j\right)\left[\frac{dw_j}{dt}\right] - \sum_{j=1}^{N} \delta'\left(I - I_j\right)\left[\frac{d\left(w_j I_j\right)}{dt} - I_j \frac{dw_j}{dt}\right] = S(I,t)$$

Both sides of Eq. (17) are multiplied by I^k for $k = 0{:}2N-1$ and integrated with respect to I from 0 to ∞ to arrive at:[35]

(18)

$$(1-k)\sum_{j=1}^{N} I_j^k \frac{dw_j}{dt} + k\sum_{j=1}^{N} I_j^{k-1} \frac{d\left(w_j I_j\right)}{dt} = \bar{S}_k$$

where the rules for delta functions are used

(19)

$$\int_0^\infty I^k \delta(I - I_j) dI = I_j^k$$

(20)

$$\int_0^\infty I^k \delta'(I - I_j) dI = -k I_j^{k-1}$$

For every value of k, Eq. (18) represents a differential equation involving $d(w_j)/dt$ and $d(w_j I_j)/dt$. Therefore, for $k = 0{:}2N - 1$, Eq. (18) represents an implicit system of $2N$ differential equations that can be solved directly for the Ntime-dependent weights, w_j, and N time-dependent nodes, I_j, of the equivalent distribution $x_I(I)$. The system of equations can be written in matrix form:[35]

(21)

$$\begin{pmatrix} 1 & \dots & 1 & 0 & \cdots & 0 \\ 0 & \dots & 0 & 1 & \dots & 1 \\ -I_1^2 & \dots & -I_N^2 & 2I_1 & \dots & 2I_N \\ \vdots & \vdots & \vdots & \vdots & \vdots & \vdots \\ 2(1-N)I_1^{2N-1} & \dots & 2(1-N)I_N^{2N-1} & (2N-1)I_1^{2N-2} & \dots & (2N-1)I_N^{2N-2} \end{pmatrix} \begin{pmatrix} dw_1/dt \\ \vdots \\ dw_N/dt \\ d(w_1 I_1)/dt \\ \vdots \\ d(w_N I_N)/dt \end{pmatrix} = \begin{pmatrix} \bar{S}_0 \\ \vdots \\ \vdots \\ \vdots \\ \bar{S}_{2N-1} \end{pmatrix}$$

The vector of moment-transformed source terms, $\bar{S}_k$, in Eq. (21) is evaluated using the quadrature approximation of Eq. (14).

Until this point, the development of DQMoM has been general and is applicable to any system governed by ordinary differential equations. The specifics of a particular problem enter via the source term, $S(I,t)$. The source term for coal tar/metaplast VLE is given by a continuous version of the right-hand-side of Eq. (5):

(22) $$S(I) = \left[\frac{(z(I)-x(I))\dot{F}}{L+VK(I)} + \frac{x(I)(1-K(I))\dot{V}}{L+VK(I)} - \frac{x(I)V}{L+VK(I)}\frac{dK(I)}{dt} + \frac{x(I)(1-K(I))}{L+VK(I)}\frac{dV}{dt}\right]$$

The transformed source terms appearing in Eq. (21) are therefore given by

(23)

$$\bar{S}_k = \int_0^\infty \left[\frac{(z(I)-x(I))\dot{F}}{L+VK(I)} + \frac{x(I)(1-K(I))\dot{V}}{L+VK(I)} - \frac{x(I)V}{L+VK(I)}\frac{dK(I)}{dt} + \frac{x(I)(1-K(I))}{L+VK(I)}\frac{dV}{dt}\right] I^k dI$$

Substituting the Gaussian quadrature approximation (Eq. (14)) into the transformed source terms in Eq. (23) and integrating yields

(24)

$$\bar{S}_k = \left(\frac{\sum_{i=1}^{n} w_i I_i^k}{L+VK_i}\right)\dot{F} - \left(\frac{\sum_{j=1}^{N} w_j I_j^k}{L+VK_j}\right)\dot{F} + \left(\frac{\sum_{j=1}^{N} w_j I_j^k (1-K_j)}{L+VK_j}\right)\dot{V} - \left(\frac{\sum_{j=1}^{N} w_j I_j^k}{L+VK_j}\frac{dK_j}{dt}\right)V + \left(\frac{\sum_{j=1}^{N} w_j I_j^k (1-K_j)}{L+VK_j}\right)\frac{dV}{dt}$$

Since the mole fraction of "feed" of fragments, z_i, is known for all discrete species from the pyrolysis decomposition scheme, the moment transform of the $z(I)$ term in Eq. (23) is evaluated using the known discrete species information, summing over discrete species $i = 1{:}n$ rather than pseudo-components $j = 1{:}N$.

In the continuous version of the model, the equation for the total liquid mole fraction is the same as in the discrete version of the model

(25) $$\frac{dL}{dt} = \dot{F} - \dot{V} - k_{cross}L - \frac{dV}{dt}$$

Similarly, V and dV/dt are still determined from the ideal gas law.

In the continuous version of the model, the total vapor molar flow rate, $\dot{V}$, is obtained from the algebraic constraint that the vapor weights sum to unity:

(26) $$\sum_j K_j w_j = 1$$

Because the model employed here is a semi-continuous model,[25] since the mole fraction of light gas is considered separately from the continuous tar distribution, the summation condition can be written as

(27)

$$y_{gas} + \sum_j K_j w_j = 1$$

DQMoM for tar vaporization can be applied with a wide variety of kinetic schemes for macromolecular decomposition, with potential extra terms present in Eq. (5).

2.3. Delumping model

Though DQMoM and other CTMs calculate the properties of an evolving distribution, information on individual species is lost. For certain problems, however, a delumping procedure can be used to combine the advantage of the full DCM with that of DQMoM: accurate calculation of every discrete species at a reduced computational cost. The delumping procedure was developed for multicomponent fuel droplets[30] and is applicable to any system of differential equations for which the nonlinearity stems from terms associated with the entire mixture. Delumping procedures for CTMs have been previously developed for systems governed by algebraic equations.[38,39]

DQMoM accurately solves for the evolution of the distribution, represented by the weights, w_j, and nodes, I_j, of its pseudo-components. Therefore, variables such as $\dot{V}$ and L which characterize the entire mixture, are computed accurately by DQMoM. Because the nonlinearity in Eq. (5) stems solely from terms representative of the mixture as a whole, if those terms are known functions of time, the system of discrete ODEs would become linear. Furthermore, any linear, first order ODE has an analytical solution in terms of integrals of the integrating factor [40]. Therefore, after solving the DQMoM version of the problem, $\dot{V}(t)$, $L(t)$ and other terms can be

substituted into discrete Eq. (5) converting it into a system of linear, first order ODEs that can be solved with the integrating factor method. Although the analytical solution requires evaluation of numerical integrals, this is computationally inexpensive compared to the solution of differential equations. In this way, the full DCM solution for every discrete species can be obtained at the cost of a CTM. It is possible to perform delumping following the DQMoM solution for the entire pyrolysis process, or following every time step of the DQMoM model.[30] The latter would be necessary if the particle pyrolysis/tar vaporization model were incorporated as a submodel for calculating species source terms in a CFD simulation.

For delumping using the integrating factor method, the differential equation for each discrete x_i (Eq. (5)) can be rearranged to combine all terms on the right-hand side involving x_i:

$$(28)\ \frac{dx_i}{dt} = \frac{z_i\dot{F}}{L+VK_i} + x_i\left[-\frac{\dot{F}}{L+VK_i} + \frac{(1-K_i)\dot{V}}{L+VK_i} - \frac{V}{L+VK_i}\frac{dK_i}{dt} + \frac{(1-K_i)}{L+VK_i}\frac{dV}{dt}\right]$$

The DQMoM solution yields $\dot{V}(t)$ and other variables that characterize the entire mixture. These known functions of time are substituted into Eq. (28), which is converted from a nonlinear differential equation, due to the dependence of $\dot{V}$ on x_i, into a linear equation in which all terms multiplying x_i are known functions of time. Note that the K_i terms are specific to each species, but do not introduce any non-linearity, since they are modeled as depending only on the temperature and molecular weight of each species, but not its mole fraction (Eq. (2)). Also note that every term is time-dependent, although not explicitly indicated.

For an ODE of the form

$$(29)\ \frac{dx}{dt} + P(t)x = Q(t)$$

the integrating factor is

$$(30)\ u(t) = exp\left[\int P(t)dt\right]$$

and the solution is given by

$$(31)\ x(t) = \frac{\int u(t)Q(t)dt + C}{u(t)}$$

For Eq. (28), for each discrete species i,

$$(32)\ P_i(t) = -\left[-\frac{\dot{F}}{L+VK_i} + \frac{(1-K_i)\dot{V}}{L+VK_i} - \frac{V}{L+VK_i}\frac{dK_i}{dt} + \frac{(1-K_i)}{L+VK_i}\frac{dV}{dt}\right]$$

$$(33)\ Q_i(t) = \frac{z_i\dot{F}}{L+VK_i}$$

The integrating factor for each species, i, is given by

(34)

$$u_i(t) = exp\left[-\int_0^t P_i(t)dt\right]$$

and the solution for each species mole fraction is given by

$$(35)\ x_i(t) = \frac{\int_0^t u_i(t)Q_i(t)dt + x_i(0)}{u_i(t)}$$

where it can be shown that the constant of integration in Eq. (31) equals the initial value $x_i(0)$.

In this way, all discrete mole fractions and fluxes can be calculated at all times using DQMoM with delumping. Because the integrating factor method is exact, the accuracy of the method is determined by the accuracy of DQMoM and the accuracy of the numerical integration in the delumping step. Although matrix exponentials can be used for integrating factors for coupled systems of linear ODEs, application of the delumping procedure is restricted to models without nonlinear terms in Eq. (5) other than those associated with the mixture as a whole. This would preclude reactions between individual metaplast species that lead to nonlinearities, such as biomolecular recombination in the liquid phase.[7]

3. Test case

3.1. Modified CPD model

To test the tar vaporization model, a method for determining the terms z_i and $\dot{F}$, which depend on the decomposition kinetics, is required. The model is tested using the CPD model for lattice statistics, decomposition kinetics and molecular fragment distribution, reformulated in rate form.[14] Terms for the "feed" stream of lumped tar fragments, $\dot{f}_{lump,k}$, are calculated on an instantaneous rate basis.[14] The calculation of the evolution of light gases employs the improved version of the CPD model of Jupudi et al.[41] with light gas evolution and initial functional group compositions based on FG-DVC.[42] The parameters used in the model are shown in Table 1 and are based on a bituminous coal.

Table 1. CPD model parameters for test case.

Parameter	Value
Coordination number, $\sigma + 1$	4.6
Initial fraction of intact labile bridges, L_0	0.61
Initial fraction of char bridges, c_0	0
Average molecular weight of cluster	267

To test the accuracy and efficiency of DQMoM for many discrete tar/metaplast species, the tar molecular fragment distribution generated by the CPD model is combined with a calculation from a Monte Carlo simulation for the discrete tar species. The purpose of this pairing is to convert the coarse $\dot{f}_{lump,k}$ from the CPD model (20 molecular weight bins, k) to a discrete $\dot{f}_i$ for many discrete species, i. The Monte Carlo calculation yielded the final counts for each of 641 discrete species with molecular weights ranging from 92 to 5822 amu, whereas the 20 fragment lumps in the CPD model are characterized by their average molecular weights, which evolve in time and have increments of roughly 300 amu. At every time step, the maximum and minimum of each of these fragment bins in the CPD model is calculated as the molecular weight halfway between a bin's average molecular weight and that of its neighbor. The instantaneous generation rate of every discrete species is then calculated as the final mole fraction of the discrete species within the bin's limits calculated by the Monte Carlo model (the bracketed term in Eq. (36)) multiplied by the instantaneous generation rate for that bin from the CPD model:

$$\dot{f}_i(t) = \dot{f}_{lump,k}(t)\left[\frac{z_{i,MC}(t_{final})}{\sum_{binmin}^{binmax} z_{i,MC}(t_{final})}\right] \quad (36)$$

The instantaneous mole fraction of each discrete species in the feed is then given by:

(37) $$z_i(t) = \frac{\dot{f}_{lump,k}(t)}{\sum_k \dot{f}_{lump,k}(t)} \left[\frac{z_{i,MC}(t_{final})}{\sum_{binmin}^{binmax} z_{i,MC}(t_{final})} \right]$$

For illustrative purposes, random fluctuations are added to the mole fraction of each species predicted by the Monte Carlo model, $z_{i,MC}(t_{final})$, because there were many heavy species for which $z_{i,MC}(t_{final})$ was identical. The total rate of fragment and gas generation is then given by

(38)
$$\dot{F} = \sum_{i=1}^{n} \dot{f}_i + \dot{f}_{gas}$$

This method of combining cumulative Monte Carlo data with instantaneous generation rates of lumped fragments is somewhat ad-hoc, but serves the purpose of testing the performance of DQMoM and delumping for pyrolysismodels with many tar species. The particle temperature for the test-case is shown in Fig. 2 and is chosen to represent conditions in a rotary reactor.

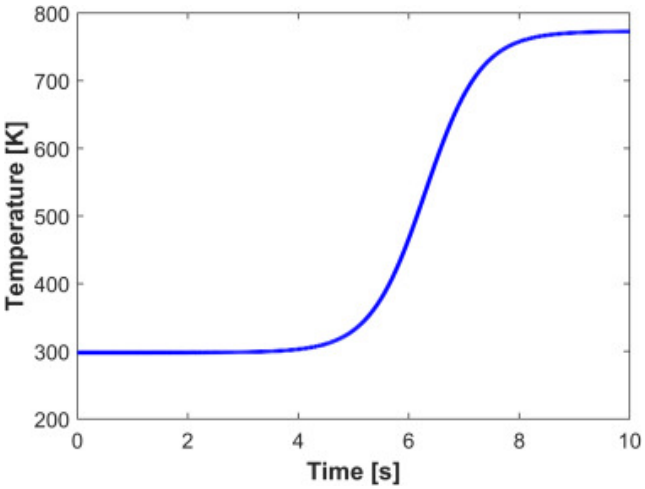

Fig. 2. Temperature vs. time for the test case.

3.2. Numerical approach

MATLAB was used to code a rate-based version of the CPD model with the generation of 641 discrete species with the DCM and DQMoM versions of the VLE submodel. Both the DCM and DQMoM versions of the models included four ODEs associated with the rate-based CPD decomposition scheme[14] and 17 additional ODEs for the light gas evolution model.[41] In addition to this computational "overhead," the DCM solved 641 ODEs for each x_i (Eq. (5)), as well as Eqs. (3), (6). DQMoM using $N = 4$ nodes solved eight ODEs for the weights and nodes of the distribution in Eq. (21), as well as Eqs. (25), (27). Integration of the differential-algebraic system was performed using the IDA solver.[43] In both the full discrete and DQMoM models the relative tolerance was 1×10^{-5}. Consistent initial condition for x_i, w_j, l_j, L and $\dot{V}$ were calculated.23 The delumping integrals were performed using the trapezoid rule. Although it is possible to perform delumping following every time step,[30] delumping was performed following integration of the entire solution from the initial to the final time.

4. Results and discussion

The accuracy and computational efficiency of DQMoM and delumping for coaltar vaporization will be compared to the full discrete model, which it seeks to approximate, and which is exact for this purpose. Typically, three or four nodes are sufficient to achieve satisfactory performance using DQMoM. The temporal evolution of the

weights and nodes for the liquid mole fraction distribution using four nodes (N = 4) are shown in Fig. 3. The weights and nodes are well-behaved, and it was verified that the weights summed to one. The time at which the nodes begin to adjust themselves to represent the evolving liquid distribution, in Fig. 3b, is the time at which pyrolysis begins in earnest.

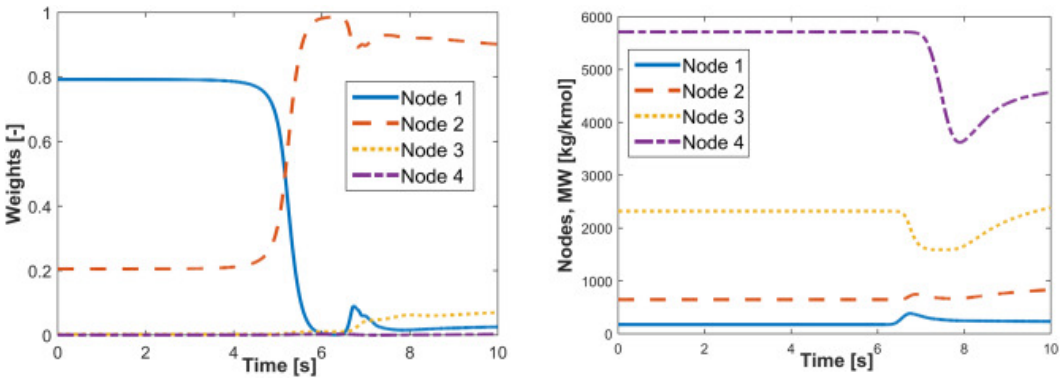

Fig. 3. Evolution of (a) weights, and (b) nodes for DQMoM with N = 4.

The performance of DQMoM is compared to the full discrete model in Fig. 4, which shows the evolution of the total vapor flow rate, $\dot{V}$, an important variable characteristic of the entire tar mixture. Excellent agreement between DQMoM and the full DCM is observed, including for the blip around 7 s, using either three or four nodes for DQMoM. Pyrolysis begins when the temperature reaches approximately 450 °C. It is noted that the figures employ the per cluster normalization of the CPD model.

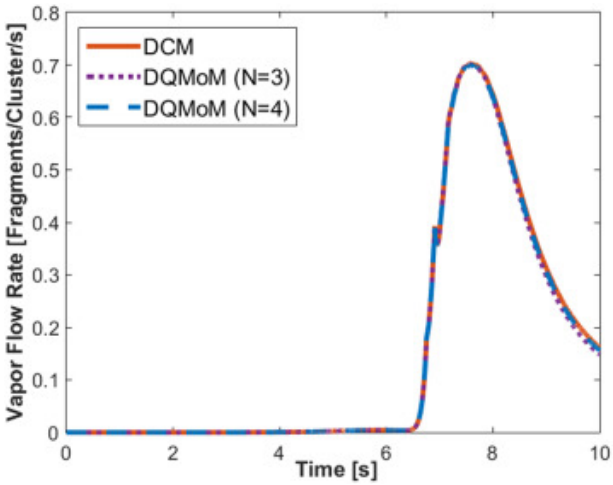

Fig. 4. Evolution of the total vapor flow rate for the full DCM and for DQMoM with N = 3 and N = 4.

Fig. 5 shows the evolution of the total accumulated liquid (metaplast), L, another variable characteristic of the entire mixture. Using four nodes, the agreement between DQMoM and the full DCM is quite good, while DQMoM using three nodes fails to capture the evolution of metaplast accumulation as accurately.

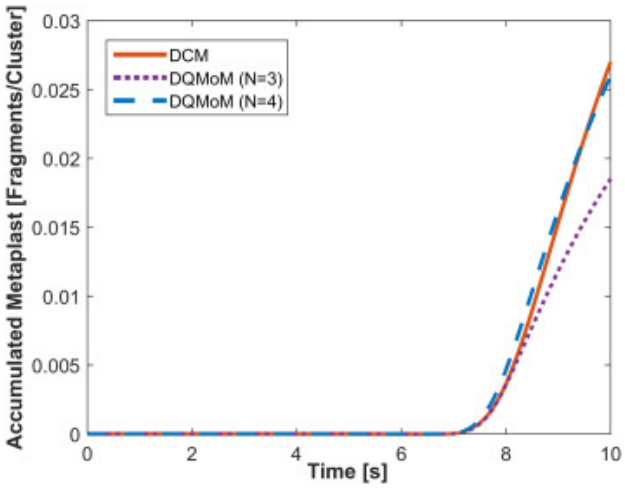

Fig. 5. Evolution of the accumulated metaplast for the full DCM and for DQMoM with N = 3 and N = 4.

The approximation of the mean molecular weight is another important characteristic to be captured by pyrolysis models. The mean metaplast molecular weight is calculated using the first moment of the liquid distribution and shown in Fig. 6. After pyrolysis begins in earnest at roughly 6.5 s, the mean molecular weight is roughly 700 kg/kmol. Using four nodes, DQMoM qualitatively captures the initial increase in mean molecular weight, its decrease beginning at 6.9 s, and its subsequent increase after 7.6 s. Quantitative agreement between DQMoM and the DCM is satisfactory, however, a discrepancy beyond 8.5 s is noted.

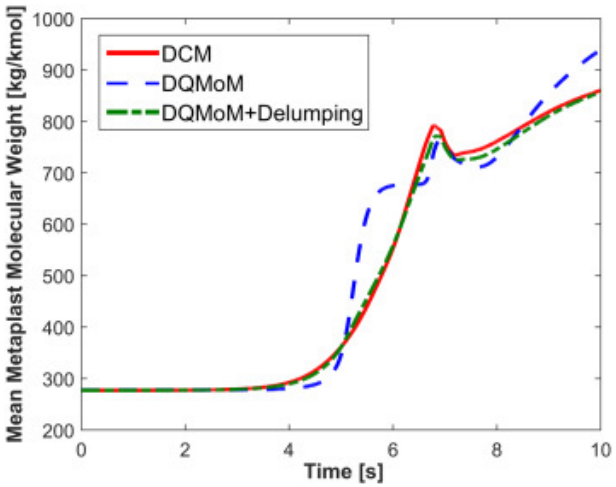

Fig. 6. Evolution of the mean metaplast molecular weight for the full DCM, for DQMoM with N = 4 and after the delumping step.

As discussed in Section 2.3, application of the delumping procedure enables calculation of variables associated with individual species from a CTM. Prior to a comparison of the detailed tar and metaplast species predictions, it is noted that the delumped solution can also be used to improve predictions for variables characteristic of the mixture as a whole, such as mean metaplast molecular weight. While stand-alone DQMoM yielded satisfactory results for this variable, Fig. 6 shows that the mean molecular weight based on the delumped solution produces good quantitative agreement with the DCM solution at all times.

Fig. 7 compares the discrete liquid mole fraction distributions calculated by DQMoM (N = 4) followed by delumping to the full DCM calculations for three times during the pyrolysis process. Although species with molecular weights up to 5822 kg/kmol are produced in small quantities, only species up to 2000 kg/kmol are shown for clarity. Agreement between the two approaches is quite good, both for the dominant metaplast

species with molecular weights below 1200 kg/kmol, as well as for heavier species present in lower concentrations, shown in the inset.

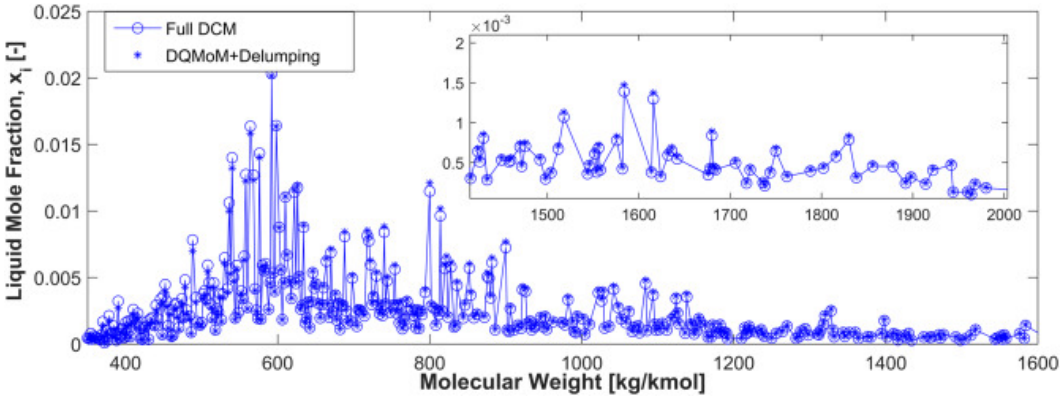

Fig. 7. Discrete metaplast mole fractions for the full DCM and DQMoM with delumping (N = 4) at 8 s.

Although the liquid mole fractions are the state variables, the flow rates of tar species are the most important discrete outputs from the model. Fig. 8 compares discrete tar vaporization rates calculated by DQMoM with delumping to those calculated by the full DCM. Excellent agreement is observed for both the lighter species that dominate the tar at these pyrolysis temperatures, as well as the heavier species that largely remain in the particle. Again, only a portion of the distribution is shown for clarity.

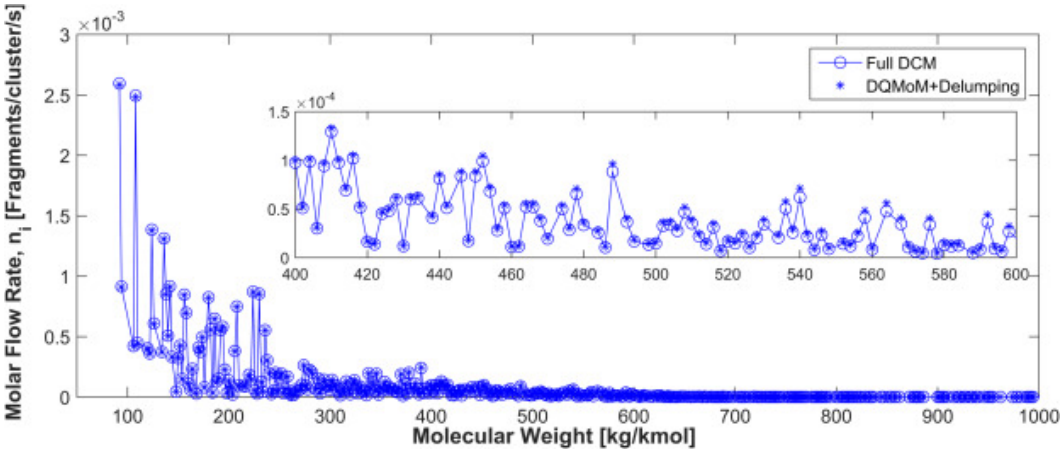

Fig. 8. Discrete tar vaporization rates for the full DCM and DQMoM with delumping (N = 4) at 8 s.

The accuracy of the delumped solution is quantified in Fig. 9, accounting for the contribution of every species as a function of time, using the relative error in the 2-norm for the approximate DQMoM with delumping, compared to the exact DCM

$$(39)\ err(t) = \frac{\left[\sum_{i=1}^{n}\left(\dot{n}^i_{DCM}(t) - \dot{n}^i_{DQMoM+delumping}(t)\right)^2\right]^{1/2}}{\left[\sum_{i=1}^{n}\left(\dot{n}^i_{DCM}(t)\right)^2\right]^{1/2}}$$

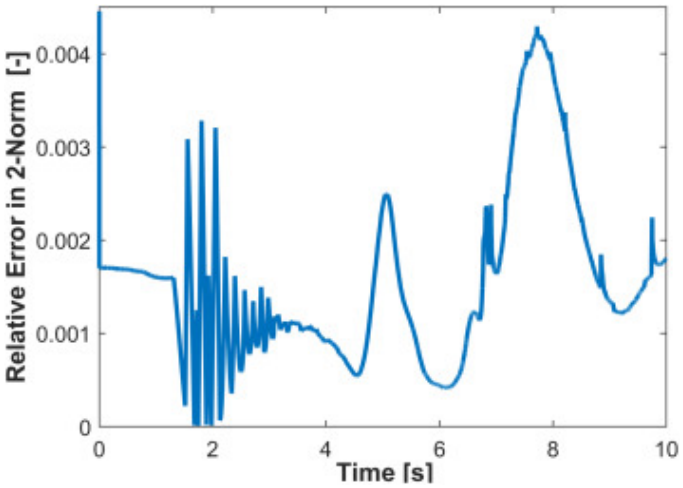

Fig. 9. Relative error in the two-norm as a function of time for DQMoM with delumping (N = 4) compared to the full DCM.

The error is < 1% at all times for DQMoM with four nodes, indicating that DQMoM with delumping produces an excellent approximation to the full discrete model.

The computational efficiency of DQMoM and delumping for N = 3 and N = 4 is compared to the full DCM in Table 2. Each entry is based on an average of three runs on a desktop machine with a single quad core processor running at 3.4 GHz. DQMoM with delumping reduces the computational cost by over 90% for the test case with 641 species. Although the computational savings would be smaller if fewer discrete tar species were modeled, it is also noted that the computational overhead associated with the 17 ODEs for light gas generation,[41] some of which are numerically stiff, decreases the CPU time reduction achieved by implementation of DQMoM. It is also noted that the delumping step typically contributes only about 5% of the computational cost of DQMoM with delumping.

Table 2. Comparison of CPU time and relative error for DQMoM with delumping (N = 3 and N = 4) and the full DCM.

	CPU time (% reduction)	Relative error (2-norm)
DCM	1080 s (−)	–
DQMoM + deluming (*N* = 3)	88.50 s (91.7%)	1.34%
DQMoM + deluming (*N* = 4)	102.90 s (90.3%)	0.57%

Despite the significant computational savings realized using DQMoM with delumping, the approach is currently too slow for CFD. For instance, the original version of the CPD model, which is often incorporated in CFD codes, runs in a fraction of a second. One potential application of the model is in simulating tar species production in coal-to-chemicals processes, in which the pyrolysis/tar vaporization model is applied to a large number of temperature histories representing different particle trajectories through realistic reactors. Such temperature-time profiles can be obtained from analysis of granular flow simulations.[44] The pyrolysis calculations might be performed for a variety of reactor operating conditions, resulting in repeated application of the tar vaporization model. The order-of-magnitude computational savings of DQMoM and delumping has the potential to alleviate what might otherwise be prohibitive calculation times in such a study.

The relative error of DQMoM with delumping, combining all discrete times, k, is also reported in Table 2, using the relative error in the 2-norm for all species and all times simultaneously

(40)

$$err = \frac{\left[\sum_{k=1}^{J} \sum_{i=1}^{n} \left(\dot{n}_{DCM}^{i,t_k} - \dot{n}_{DQMoM+delumping}^{i,t_k}\right)^2\right]^{1/2}}{\left[\sum_{k=1}^{J} \sum_{i=1}^{n} \left(\dot{n}_{DCM}^{i,t_k}\right)^2\right]^{1/2}}$$

This metric accounts for the fact that minimal pyrolysis occurs at early times and that many species are present in lesser amounts. With relative errors below 2%, it is concluded that DQMoM with delumping is an accurate and computationally efficient alternative to full discrete component models.

5. Conclusions

DQMoM is proposed for efficient modeling of tar vaporization during coal particle pyrolysis without assuming any functional form for the distribution of tar or metaplast species. Using just four nodes and weights to represent a mixture of 641 species, DQMoM has been shown to accurately predict the evolution of total tar and light gas vaporization rates, the accumulation of metaplast and other characteristics of the species distribution, such as mean molecular weight. The DQMoM approach for multicomponent VLE can be combined with a variety of kinetic decomposition mechanisms that might be employed for coal pyrolysis. Although demonstrated here for a multicomponent VLE formulated as a DAE system, DQMoM can also be applied to a computationally simpler ODE formulation.

A delumping procedure has also been applied to recover information on the instantaneous tar vapor fluxes and metaplast mole fractions for every discrete species. Delumping is applicable whenever the nonlinearity in the governing equations is associated with the mixture as a whole. This is the case for the extended CPD model[3] and for models based on lumped fragment species parametrized by Monte Carlo or molecular dynamics results, such as the test case presented, but not for models in which molecular fragments react with one another in the liquid phase producing nonlinear terms. The combination of DQMoM with delumping was compared to a full DCM and excellent agreement was obtained for the 641 discrete mole fractions and tar vaporization rates, with substantial computational savings.

Nomenclature

C constant in Eq. (31)
$f(I)$ function multiplying weight function in Eq. (13)
$\dot{F}$ molar flow rate of feed
I distribution variable (molecular weight)
K_i equilibrium constant
k_{cross} CPD rate constant for cross-linking
L moles total liquid (metaplast)
l_i moles of liquid species i
m_k kth moment
MW molecular weight
N number of nodes
N number of discrete species
P pressure
$P(t)$ function in Eq. (29)
$Q(t)$ function in Eq. (29)
S source term
T temperature
t time

$u(t)$ integrating factor
V moles total vapor
$\dot{V}$ total molar flow rate of vapor
v_i moles of vapor species i
w_j weight
x liquid mole fraction
y vapor mole fraction
z feed mole fraction
α parameter in vapor pressure correlation
β parameter in vapor pressure correlation
γ parameter in vapor pressure correlation

Subscripts

Gas light gas
Final at the final time
i discrete species index
j node index
k moment order index, or fragment index in Eqs. (36), (37), or timestep index in Eq. (40)
lump CPD fragment
MC Monte Carlo
tot total (for all species or nodes)
v vapor

Acknowledgments

The authors would like to thank Prof. William Green of the Chemical Engineering department at MIT for helpful comments on the manuscript, and Prof. Jianghuai Cai of the Aerospace department at Xiamen University for supplying the Monte Carlo simulation results for the test case. This research did not receive any specific grant from funding agencies in the public, commercial, or not-for-profit sectors.

References

[1]H.H. Schobert, C. Song. **Chemicals and materials from coal in the 21st century.** Fuel, 81 (2002), pp. 15-32, 10.1016/S0016-2361(00)00203-9

[2]M. Granda, C. Blanco, P. Alvarez, J.W. Patrick, R. Menéndez **Chemicals from coal coking.** Chem. Rev., 114 (2014), pp. 1608-1636, 10.1021/cr400256y

[3]S. Umemoto, S. Kajitani, K. Miura, H. Watanabe, M. Kawase **Extension of the chemical percolation devolatilization model for predicting formation of tar compounds as soot precursor in coal gasification.** Fuel Process. Technol., 159 (2017), pp. 256-265, 10.1016/j.fuproc.2017.01.037

[4]D.B. Anthony, J.B. Howard, H.C. Hottel, H.P. Meissner **Rapid devolatilization of pulverized coal** Symp. Combust., 15 (1975), pp. 1303-1317, 10.1016/S0082-0784(75)80392-4

[5]S. Niksa, G. Liu, R.H. Hurt **Coal conversion submodels for design applications at elevated pressures. Part I. Devolatilization and char oxidation** Prog. Energy Combust. Sci., 29 (2003), pp. 425-477, 10.1016/S0360-1285(03)00033-9

[6]D.M. Grant, R.J. Pugmire, T.H. Fletcher, A.R. Kerstein **Chemical model of coal devolatilization using percolation lattice statistics** Energy Fuel, 3 (1989), pp. 175-186, 10.1021/ef00014a011

[7]S. Niksa, A.R. Kerstein **Flashchain theory for rapid coal devolatilization kinetics. 1. Formulation** Energy Fuel, 5 (1991), pp. 647-665, 10.1021/ef00029a006

[8]P.R. Solomon, D.G. Hamblen, R.M. Carangelo, M.A. Serio, G.V. Deshpande **General model of coal devolatilization** Energy Fuel, 2 (1988), pp. 405-422

[9]S. Niksa **Rapid coal devolatilization as an equilibrium flash distillation** AIChE J, 34 (1988), pp. 790-802, 10.1002/aic.690340509
[10]T.H. Fletcher, A.R. Kerstein, R.J. Pugmire, D.M. Grant **Chemical percolation model for devolatilization. 2. Temperature and heating rate effects on product yields** Energy Fuel, 4 (1990), pp. 54-60
[11]T.H. Fletcher, A.R. Kerstein, R.J. Pugmire, M. Solum, D.M. Grant **A chemical percolation model for devolatilization: summary** Sandia Report SAND92-8207 (1992)
[12]S. Niksa **Modeling the devolatilization behavior of high volatile bituminous coals, twenty-second** Symp. Combust., 22 (1988), pp. 105-114
[13]R.L. Cotterman, R. Bender, J.M. Prausnitz **Phase equilibria for mixtures containing very many components. Development and application of continuous thermodynamics for chemical process design** Ind. Eng. Chem. Process. Des. Dev., 24 (1985), pp. 194-203, 10.1021/i200028a033
[14]S. Singer, J. Cai, W.H. Green **Detailed modeling of pyrolysis of large lignite particles** Clearwater Coal Conf (2015)
[15]M. Zheng, X. Li, J. Liu, L. Guo **Initial chemical reaction simulation of coal pyrolysis via ReaxFF molecular dynamics** Energy Fuel, 27 (2013), pp. 2942-2951, 10.1021/ef400143z
[16]M. Zheng, X. Li, J. Liu, Z. Wang, X. Gong, L. Guo, *et al.* **Pyrolysis of liulin coal simulated by GPU-based ReaxFF MD with cheminformatics analysis** Energy Fuel, 28 (2014), pp. 522-534, 10.1021/ef402140n
[17]F. Castro-Marcano, M.F. Russo, A.C.T. Van Duin, J.P. Mathews **Pyrolysis of a large-scale molecular model for Illinois no. 6 coal using the ReaxFF reactive force field** J. Anal. Appl. Pyrolysis, 109 (2014), pp. 79-89, 10.1016/j.jaap.2014.07.011
[18]J.P. Mathews, A.L. Chaffee **The molecular representations of coal – a review** Fuel, 96 (2012), pp. 1-14, 10.1016/j.fuel.2011.11.025
[19]F. Castro-Marcano, V.V. Lobodin, R.P. Rodgers, A.M. McKenna, A.G. Marshall, J.P.Mathews **A molecular model for Illinois No. 6 Argonne Premium coal: moving toward capturing the continuum structure** Fuel, 95 (2012), pp. 35-49, 10.1016/j.fuel.2011.12.026
[20]G.R. Gavalas, P.H. Cheong, R. Jaln **Model of coal pyrolysis. 1. Qualitative development** Ind. Eng. Chem. Fundam. (1981), pp. 113-122
[21]T. Fletcher, D.M. Grant, R. Pugmire **Predicting vapor pressures of tar and metaplast during coal pyrolysis** ACS Div. Fuel Chem., 36 (1991), pp. 250-257 http://www.anl.gov/PCS/acsfuel/preprintarchive/Files/Merge/Vol-36_1-0001.pdf
[22]E.R.A. Lima, M. Castier, C.B. Evaristo Jr. **Differential-algebraic approach to dynamic simulations of flash drums with rigorous evaluation of physical properties** Oil Gas Sci. Technol. – Rev. d'IFP Energies Nouv., 63 (2008), pp. 677-686, 10.2516/ogst
[23]J.R. Cash **Efficient numerical methods for the solution of stiff initial-value problems and differential algebraic equations efficient numerical methods for the solution** Proc. R. Soc. Lond. A Math. Phys. Sci., 459 (2003), pp. 797-815, 10.1098/rspa.2003.1130
[24]S. Niksa **FLASHCHAIN theory for rapid coal devolatilization kinetics. 2. Impact of operating conditions** Energy Fuel, 34 (1991), pp. 665-673
[25]R.L. Cotterman, J.M. Prausnitz **Adiabatic flash calculations for continuous or semicontinuous mixtures using an equation of state** Ind. Eng. Chem. Process. Des. Dev., 24 (1985), pp. 434-443, 10.1016/0378-3812(86)80043-7
[26]P.L.C. Lage **The quadrature method of moments for continuous thermodynamics** Comput. Chem. Eng., 31 (2007), pp. 782-799, 10.1016/j.compchemeng.2006.08.005
[27]R. McGraw **Description of aerosol dynamics by the quadrature method of moments** Aerosol Sci. Technol., 27 (1997), pp. 255-265, 10.1080/02786829708965471
[28]A. Bruyat, C. Laurent, O. Rouzaud **Direct quadrature method of moments for multicomponent droplet spray vaporization** 7th Int. Conf. Multiph. Flow (2010), pp. 51-59
[29]D.L. Marchisio, R.O. Fox **Solution of population balance equations using the direct quadrature method of moments** J. Aerosol Sci., 36 (2005), pp. 43-73, 10.1016/j.jaerosci.2004.07.009

[30]S.L. Singer **Direct quadrature method of moments with delumping for modeling multicomponent droplet vaporization** Int. J. Heat Mass Transf., 103 (2016), pp. 940-954
[31]A.Y. Cooney, S.L. Singer **Modeling multicomponent fuel droplet vaporization with finite liquid diffusivity using Coupled Algebraic-DQMoM with delumping** Fuel, 212 (2018), pp. 554-565, 10.1016/j.fuel.2017.10.056
[32]D.L. Marchisio, J.T. Pikturna, R.O. Fox, R.D. Vigil **Quadrature method of moments for population balance equations** AIChE, 49 (2003), pp. 1266-1276, 10.1002/aic.690490517/abstract
[33]D.L. Marchisio, R.D. Vigil, R.O. Fox **Quadrature method of moments for aggregation-breakage processes** J. Colloid Interface Sci., 258 (2003), pp. 322-334, 10.1016/S0021-9797(02)00054-1
[34]C. Laurent, G. Lavergne, P. Villedieu **Quadrature method of moments for modeling multi-component spray vaporization** Int. J. Multiphase Flow, 36 (2010), pp. 51-59, 10.1016/j.ijmultiphaseflow.2009.08.005
[35]D.E. Marchisio, R.O. Fox (Eds.), Multiphase Reacting Flows: Modeling and Simulation, Springer Wien, New York (2007)
[36]R.G. Gordon **Error bounds in equilibrium statistical mechanics** J. Math. Phys., 9 (1968), pp. 655-663, 10.1063/1.1664624
[37]J.C. Wheeler **Modified moments and Gaussian quadratures** Rocky Mt. J. Math., 4 (1974), pp. 287-296, 10.1216/RMJ-1974-4-2-287
[38]D.V. Nichita, C.F. Leibovici **An analytical consistent pseudo-component delumping procedure for equations of state with non-zero binary interaction parameters** Fluid Phase Equilib., 245 (2006), pp. 71-82, 10.1016/j.fluid.2006.03.016
[39]M. Petitfrere, D.V. Nichita, F. Montel **Multiphase equilibrium calculations using the semi-continuous thermodynamics of hydrocarbon mixtures** Fluid Phase Equilib., 362 (2014), pp. 365-378, 10.1016/j.fluid.2013.10.056
[40]C.H. Edwards, D.E. Penney **Differential Equations and Boundary Value Problems** (2nd ed.), Prentice-Hall, Upper Saddle River, New Jersey (2000)
[41]R.S. Jupudi, V. Zamansky, T.H. Fletcher **Prediction of light gas composition in coal devolatilization** Energy Fuel, 23 (2009), pp. 3063-3067, 10.1021/ef9001346
[42]M.A. Serio, D.G. Hamblen, J.R. Markham, P.R. Solomon **Kinetics of volatile product evolution in coal pyrolysis: experiment and theory** Energy Fuel, 1 (1987), pp. 138-152
[43]A.C. Hindmarsh, P.N. Brown, K.E. Grant, S.L. Lee, R. Serban, D.A.N.E. Shumaker, *et al.* **SUNDIALS: suite of nonlinear and differential/algebraic equation solvers** ACM Trans. Math. Softw., 31 (2005), pp. 363-396, 10.1145/1089014.1089020
[44]B. Yohannes, H. Emady, K. Anderson, I. Paredes, M. Javed, W. Borghard, *et al.* **Scaling of heat transfer and temperature distribution in granular flows in rotating drums** Phys. Rev. E Stat. Nonlinear Soft Matter Phys., 94 (2016), pp. 1-5, 10.1103/PhysRevE.94.042902